AIP | The Journal of Chemical Physics

Reaction of CF3 radicals on fused silica between 320 and 530 K

N. Selamoglu, M. J. Rossi, and D. M. Golden

Citation: The Journal of Chemical Physics **84**, 2400 (1986); doi: 10.1063/1.450836
View online: http://dx.doi.org/10.1063/1.450836
View Table of Contents: http://scitation.aip.org/content/aip/journal/jcp/84/4?ver=pdfcov
Published by the AIP Publishing

Reaction of CF_3 radicals on fused silica between 320 and 530 K[a]

N. Selamoglu,[b] M. J. Rossi, and D. M. Golden
Department of Chemical Kinetics, SRI International, Menlo Park, California 94025

(Received 8 October 1985; accepted 4 November 1985)

The reaction between CF_3 radicals and silicon oxide (fused silica) surface was studied in a VLPΦ flow reactor ($\sim$0.1–3 mTorr) as functions of surface temperature (320–530 K) and CF_3 concentration. The CF_3 radicals were generated from CF_3I by CO_2 laser photolysis, and the subsequent gas-phase reaction products were followed by mass spectroscopy. The surface reaction was found to yield CO, HF, CO_2, COF_2, and SiF_4. It was found that H_2O residing on the silicon oxide surface was largely responsible for the oxygen- and hydrogen-containing products, and that little etching of the SiO_2 itself occurred under these conditions. The rates for the irreversible surface loss of CF_3, and for the formation of CO were both first order with respect to $[CF_3]$. These were found to be temperature dependent with $E_a \simeq 4.7$ and 7.5 kcal/mol, respectively. The CF_3 surface loss rate indicates that the sticking coefficient for this radical on quartz is between 0.0014–0.017 for the temperature range of this study.

I. INTRODUCTION

In the plasma etching of semiconductor materials, it is known that neutrals as well as charged species play roles in the etching process.[1–3] Neutrals, such as atoms and radicals, etch the substance of interest isotropically while ion bombardment produces anisotropic etching. In general, the etching process must involve the following: chemical adsorption of the active species on the surface, rearrangement of the reactant–surface intermediate to yield etch products, and the removal of volatile etch products from the surface by desorption. Ion bombardment may assist neutral etching in various ways, such as by preparing a clean surface prior to the adsorption step, or by desorbing products from the surface, as well as possibly affecting the chemistry.

The extreme complexity of plasma systems involving atoms, radicals, ions, and electrons makes it difficult to extract fundamental mechanistic information on the process. In order to assess the importance of various neutral and ionic reactions, model experiments must be carried out under controlled conditions. Among these are studies where atoms or radicals are generated either photochemically or by a discharge, and then reacted with the surface of interest[4–8] as well as beam studies on ion–surface interactions.[9,10] The etching of silicon and silicon oxide by F atoms has been studied extensively,[4–7] and it has been found that F atoms selectively and efficiently etch silicon. In the etching of silicon oxide, however, fluorocarbon radicals, such as CF_2 and CF_3, are expected to play an important role, according to results from plasma etching studies. The reactivities of CF_2 and CF_3 radicals with Si and SiO_2 have been studied under nonionic conditions where the surfaces of interest were irradiated with the same UV excimer laser beam generating the radicals.[4,8] In these high pressure (10–500 Torr) studies, it was found that CF_2 etches SiO_2 efficiently while CF_3 has poor efficiency.

The motivation for the present study was to fill a gap between various studies ranging from complex plasma systems to ultrahigh vacuum beam studies. The purpose was to investigate the reactivity of CF_3 on a fused silica surface at pressures and radical concentrations resembling those in plasma etchers ($<$ 10 mTorr total pressure, 10^{11}–10^{13} radicals cm^{-3}). Unlike in beam studies of ion–surface interactions, the substrate was not intended to be a well-characterized clean surface but rather to be under conditions of "practical" interest. In this work, a CO_2 laser beam was used to generate radicals but not to irradiate the surface. The surface temperature could be varied between 25 and 300 °C.

The VLPΦ (very low-pressure photolysis) method used for this investigation is a well-established technique[11–13] for the kinetic study of homogeneous gas-phase reactions and is used here for the first time to study radical–surface interactions. (Variations in which radicals were generated via microwave discharge have been used in the past.[14]) Due to the importance of gas–wall collisions inherent in the method, it is almost always necessary to deactivate the vessel walls when studying homogeneous gas-phase processes. This disadvantage from the viewpoint of gas-phase chemistry makes it possible to study gas–surface chemistry by VLPΦ. In the latter, the vessel walls are again deactivated, but this time, the active surface of interest is placed in the vessel and exposed to the reactant. Reactants and products are monitored mass spectrometrically.

The method yields not only qualitative information on the gas-phase product spectrum but also quantitative information on reaction rates. The latter include the rate of consumption of CF_3 radicals on the silica surface and the rates of formation of products as functions of the surface temperature. These data allow the determination of CF_3 sticking coefficients on fused silica as functions of temperature.

II. EXPERIMENTAL

The VLPΦ technique utilizes a low-pressure ($<$10 mTorr) Knudsen flow reactor, where molecular flow condi-

---

[a] This work was supported by the Air Force Office of Scientific Research, Contract No. F49620-83-K-0001.

[b] Postdoctoral research associate.

tions are maintained. The reactor used in our measurements is shown in Fig. 1. The radical precursor CF_3I flows into the Knudsen cell where it resides for 1.7 s, before it effuses out of the exit aperture and into the mass spectrometric detection area. Decomposition to form CF_3 is effected by a CO_2 laser. The fate of the CF_3 radicals is then either to recombine, yielding C_2F_6, or to escape from the reactor. The collision number of 1.3×10^4 with the reactor walls ensures thermalization of the CF_3 radicals before any of the above reactions take place. In the event that an active surface is present in the cell, as is the case in this study, CF_3 may also undergo gas–surface reaction during the time it strikes that surface. (The collision frequency for the active surface is 600 s^{-1}.) The gas-phase products leaving the reactor are formed into an effusive molecular beam which is monitored mass spectrometrically, and the rates of the chemical reactions are obtained with respect to the known escape rate. The VLPΦ method may be carried out under steady-state or under single-pulse irradiation conditions. In this particular study, a high repetition rate (20 Hz) laser was used: since the time between pulses is shorter than the residence time or typical times for reaction (seconds), species' concentrations are maintained at close to steady-state conditions.

The processes involving CF_3 in the VLPΦ reactor are summarized in the following scheme:

$$CF_3I \xrightarrow{nh\nu} CF_3 + I\,, \tag{1}$$

$$CF_3 + CF_3 \xrightarrow{k_r} C_2F_6\,, \tag{2}$$

$$CF_3 \xrightarrow{k_e} \text{escape out of reactor}\,, \tag{3}$$

$$CF_3 + S \xrightarrow{k_w} \text{irreversible surface loss}\,. \tag{4}$$

Step (1) represents the IR-laser multiphoton decomposition forming CF_3 while (2) is the homogeneous gas-phase recombination[15] forming C_2F_6. Loss of CF_3 other than by recombination include escape (3) and surface reaction (4).

Under steady-state conditions the above mechanism leads to the following expression:

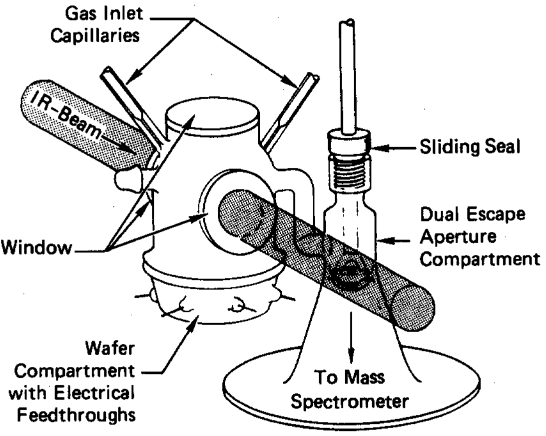

FIG. 1. Low-pressure photolysis cell for the investigation of free radical–surface interactions. The 2 in. diameter fused-silica flat lies horizontally in the wafer compartment.

$$f(F^i_{CF_3I})/(F^o_{C_2F_6}) = 2 + (k_e + k_w)k_r^{-1/2}V^{1/2}F^o_{C_2F_6}{}^{-1/2}\,, \tag{5}$$

where $F^i_{CF_3I}$ is the flow rate of CF_3I into the reactor, $F^o_{C_2F_6}$ is the C_2F_6 flow rate out of the reactor, V is the volume, and f is the fractional depletion in the steady-state CF_3I signal when the sample is irradiated. Thus, with the appropriate measurements of $F^i_{CF_3I}$, f, and $F^o_{C_2F_6}$, in conjunction with the known k_e and k_r, the CF_3 surface loss rate constant k_w may be obtained.

In fact, two methods were used to generate the CF_3 radicals from the CF_3I percursor: (a) CO_2 laser IR-multiphoton decomposition and (b) hot wire decomposition. The laser experiments led to quantitative kinetic studies. The hot-wire experiments were designed to obtain qualitative information on the origin of products. A hot nichrome wire (800–1000 °C) effected CF_3I decomposition in the latter experiments.

Experiments consisted of flowing CF_3I through the reactor and measuring steady-state mass spectrometric signals of CF_3I and of stable gas-phase reaction products. These were followed with laser on/off, as functions of CF_3I flow rate and of substrate temperature.

The parameters for the VLPΦ reactor are: $V = 250\ cm^3$; reactor wall area $= 420\ cm^2$; IR-beam pathlength $= 10$ cm. The escape rate constant for species with molecular weight, M, is given by $k_e(M) = 0.475\,(T/M)^{1/2}$. The Pyrex reactor was gold coated (Engelhard Industries) to minimize wall losses. The fused silica substrate (2 in. diameter) rested on a heated stainless-steel block in the wafer compartment, and its temperature was monitored using a thermocouple.

A Tachisto 555 CO_2 laser was used with the following irradiation conditions: $\bar{\nu} = 1076\ cm^{-1}$ [9.6 $R(16)$ line], pulse repetition rate $= 20$ Hz, beam diameter $= 1.1$ cm, fluence $= 0.8\ J/cm^2$; fractional dissociation per pulse in irradiated volume $= 3\%–12\%$.

The molecular beam effusing from the cell was chopped by means of a tuning fork chopper and analyzed using a Balzers 311 quadrupole mass spectrometer. The technique discriminates against all background gases not originating from the cell. Mass spectral calibrations of signal versus flow rate were carried out for all the compounds of interest.

III. RESULTS AND DISCUSSION

A. Origin of Products

Typical experimental traces of the mass spectrometric signal of reactant and products, with laser on/off are shown in Fig. 2. The observable gas-phase products from the reaction of CF_3 with fused silica are CO, HF, CO_2, COF_2, and SiF_4, in decreasing order of importance. In fact, the CO and HF are approximately 25–100 times larger in quantity than the other products. SiF_4 is the least important, about 100 times less than CO. These products all come from a surface reaction on the fused silica. The actual yields are not exactly reproducible over several weeks' measurements, however, general trends are reproducible. This is attributed to changing conditions on the surface. In addition to the surface reaction products there is the competing gas-phase recombination product C_2F_6. All of the products are observed only in

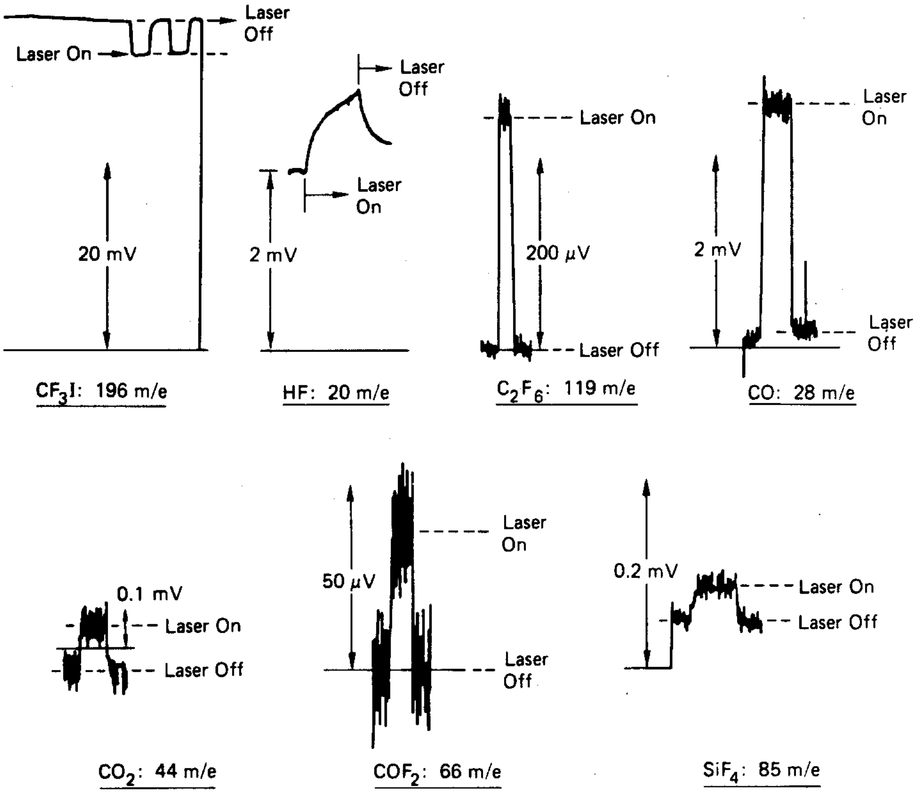

FIG. 2. Mass spectrometric data from laser experiments. Pulse repetition rate = 20 Hz. $F^{i}_{CF_3I} = 8\times10^{15}\,s^{-1}$. $T_{SiO_2} = 230\,^{\circ}C$. The figure shows signals as functions of time as laser is turned on and off.

the presence of CF_3I and with laser irradiation, thus ruling out the possibility of CF_3I undergoing dissociative adsorption on the surface. (This is equivalent to a CF_3I sticking coefficient, γ, of less than 10^{-5} given our detection sensitivity.)

The origin of HF has to be elucidated first, since neither the reactant nor the substrate compositions contain any hydrogen. Another question concerns the balance of Si versus O in the reaction products. The only Si-containing product SiF_4 occurs in quantities $\sim$100–200 times smaller than the O-containing products CO, CO_2, COF_2, most of which is comprised by CO. If the oxygen in CO were coming directly from SiO_2, then we would expect much more SiF_4 than observed to make up the balance, because SiF_4 was the only Si-containing product under our experimental conditions.

In all of our mass spectra, we noticed the presence of H_2O in the cell background. The H_2O is independent of the laser and of the CF_3I flow, but may show some variation from day-to-day. We believe the water originates from the bulk glass, i.e., the silica substrate and the Pyrex reactor. The mass spectral signals indicate apparent H_2O flow rates between 10^{14} and $10^{15}\,s^{-1}$, depending on the substrate temperatures. In hot-wire experiments with CF_3I, we noticed that the heating of the wire and the formation of HF was accompanied by a noticeable decrease in the H_2O, suggesting that the source of HF was H_2O. This was clarified by experiments where D_2O was deliberately flowed into the cell, ($F^{i}_{D_2O} = 3\times10^{15}\,s^{-1}$, $F^{i}_{CF_3I} = 1.1\times10^{15}\,s^{-1}$). As expected, DF was seen in appreciable quantities ($F^{o}_{DF} \sim 8\times10^{14}\,s^{-1}$), confirming that the origin of HF was indeed H_2O. The fact that the flux of HF or DF out of the Knudsen cell is small can be attributed to the well-known tendency of HF to physisorb to glass and metal surfaces. Once the source of HF is turned off, the flux lingers on for hours so that HF cannot be used as a probe for the surface reaction in a convenient way.

In addition to producing DF, the presence of D_2O affected the other products. CO showed a factor of 1.7 increase, while SiF_4 decreased by a factor of $\sim$3, as did C_2F_6 (see Fig. 3). That CO increases in the presence of D_2O suggests that some of the CO may originate from water. We shall address this question below with oxygen-isotope measurements. The decrease in SiF_4 with D_2O may come about because (1) the SiF_4 product reacts with D_2O, or (2) in the presence of D_2O, there is less CF_3 available for the etching reaction to produce SiF_4, due to reaction of CF_3 with D_2O. Under our conditions, possibility (1) is not important. Control experiments were carried out with small flow rates of SiF_4 and H_2O at various substrate temperatures. The SiF_4 signal did not show any dependence on the presence of water. Explanation (2) accounts for the depletion in SiF_4: The SiO_2 and the surface H_2O compete against each other for reaction with CF_3. When H_2O or D_2O is present, there is less available CF_3 for the SiO_2 etching reaction thereby decreasing SiF_4. Since there is less CF_3 available for the recombination reaction as well, we see a decrease also in the C_2F_6 yield when water is present [Fig. 3(c)]. Thus, the etching reaction is inhibited by the presence of water.

Next, H_2O^{18} experiments were performed in order to find the source of oxygen in the O-containing products CO, CO_2, and COF_2, the two possible sources being SiO_2 and H_2O. Labeled H_2O^{18} was flowed through the reactor for several hours and allowed to equilibrate before measurement. The mass spectrum of the products revealed the presence of

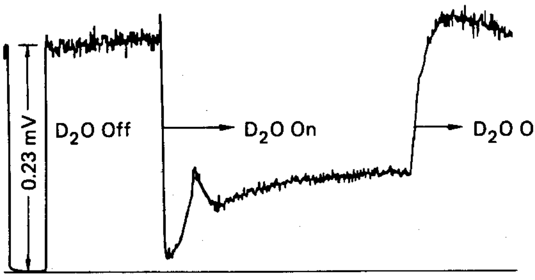

(a) SiF_4

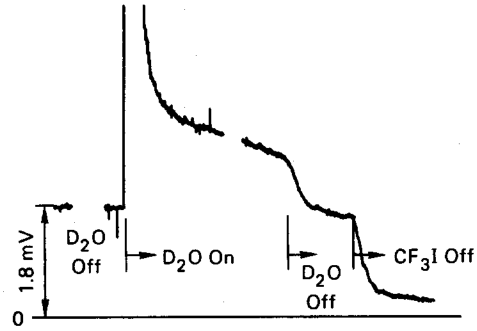

(b) CO

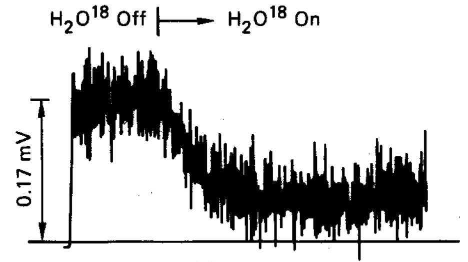

(c) C_2F_6

FIG. 3. Effect of water on products in hot-wire experiments. (a) SiF_4 signal at 85 m/e. $F^i_{CF_3I} = 1.1\times10^{15}\,s^{-1}$; $F^i_{D_2O} \cong 3\times10^{15}\,s^{-1}$; $T_{SiO_2} = 145$ °C. (b) CO signal at 28 m/e. Other conditions given in (a). (c) C_2F_6 signal at 119 m/e. $F^i_{CF_3I} = 1.4\times10^{15}\,s^{-1}$; $F^i_{H_2O^{18}} \cong 1\times10^{15}\,s^{-1}$; $T_{SiO_2} = 100$ °C.

all isotopic combinations: CO^{18}, CO_2^{18}, $CO^{18}O^{16}$, and $CO^{18}F_2$ appeared in addition to CO^{16}, CO_2^{16}, and $CO^{16}F_2$. The quantitative results are shown in Table I. Notice that the abundance of each isotopic composition agrees with the H_2O^{18}/H_2O^{16} ratio. In the case of CO_2, where two oxygens are present, the CO_2^{16}: $CO^{18}O^{16}$:CO_2^{18} ratios follow the probability rule $(H_2O^{16})^2$: $2(H_2O^{16}*H_2O^{18})$:$(H_2O^{18})^2$ very well.

The good agreement between the product ratios and the H_2O^{18}/H_2O^{16} ratio indicates that almost all of the CO, CO_2, and COF_2 come from the reaction of CF_3 with water, and that the contribution from $CF_3 + SiO_2$ is very small indeed. Furthermore, if the latter had been important, a considerable amount of SiF_4 would have to be expected in order to account for the silicon. Since we have very little SiF_4 in our measurements, this supports the conclusion that the SiO_2 etching reaction is not as important as the $CF_3 + H_2O$ reaction under our conditions. It should be emphasized that while the majority of the reaction is traced to water, this is a surface reaction consuming CF_3 and occurring on the fused silica surface, because the reaction products are only observable when CF_3 radicals strike the heated surface.

B. Kinetics

Figures 4, 5, and 6 show product concentrations as functions of $[CF_3]_0$ for the laser experiments. $[CF_3]_0$ is the steady-state CF_3 concentration that would be available if there were no chemical losses [given by $(f*F^i_{CF_3I})/(V*k_e)$]. Notice that all products show positive dependence on the CF_3 concentration. Notice in Figs. 4 and 5 that for a given $[CF_3]_0$, increasing temperature affects $[C_2F_6]$ and [CO] in different ways. CO, representative of the surface reaction, increases with temperature while C_2F_6 decreases. This suggests that at the higher surface temperatures the rates for the surface reactions increase, thereby throttling off the gas-phase recombination reaction. The other surface-related products, CO_2, COF_2, and SiF_4 show temperature dependence similar to CO (not shown in figure).

The temperature dependence may be seen more clearly in Fig. 7 showing the dependence of the product yields on substrate temperature with constant CF_3I flow rate. Notice the strong increase in surface-related products CO, CO_2, HF, SiF_4, and COF_2 with temperature. We associate the increased yields of the surface-related products with strongly temperature-dependent surface-reaction rates. The decrease in the surface product COF_2 at the high temperatures is attributable to decomposition of that product following its formation on the surface. By contrast, the decrease in the C_2F_6 yield at the higher temperatures is ascribed to a competition effect: the strongly temperature-dependent surface reaction competes against the nearly temperature independent gas-phase recombination for the available CF_3 radicals, thereby decreasing the C_2F_6 yield. These experiments are, in fact, not as straightforward as intended because the extent of decomposition f, and therefore $[CF_3]_0$, are temperature dependent as well, as is the reaction. The variation of f with temperature is shown in the inset in Fig. 7(a). Thus, these experiments were performed under conditions where $[CF_3]_0$ and T_{SiO_2} were both changing and affecting reaction rates.

TABLE I. Oxygen-isotope abundances of products CO, CO_2, and COF_2 in hot-wire experiments with H_2O^{18}.[a]

Species	H_2O^{16}	H_2O^{18}	CO^{16}	CO^{18}	CO_2^{16}	$CO^{16}O^{18}$	CO_2^{18}	$CO^{16}F_2$	$CO^{18}F_2$
m/e	18	20	28	30	44	46	48	47	49
S(mV)	3.92	4.55	2.8	3.0	0.20	0.48	0.26	0.04	0.04
Ratio	1.0 :	1.16	1.0 :	1.07	1.0 :	2.4 :	1.3	1 :	1

[a] $F^i_{H_2O^{18}} \cong 1.0\times10^{15}\,s^{-1}$. $T_{SiO_2} = 100$ °C. $F^i_{CF_3I} = 1.4\times10^{15}\,s^{-1}$. (Increasing $F^i_{CF_3I}$ from 1.4×10^{15} to $8.2\times10^{15}\,s^{-1}$ increased the product yields but did not change the isotopic ratios.)

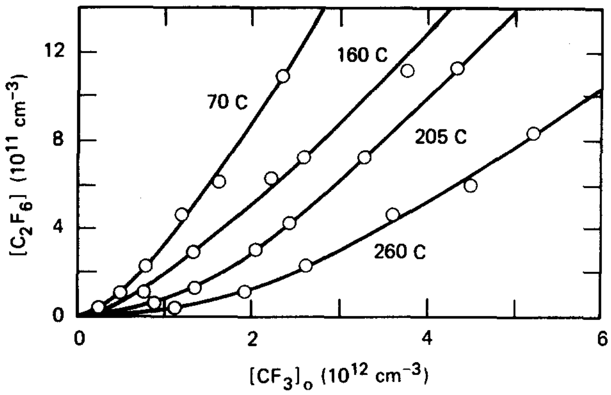

FIG. 4. $[C_2F_6]$ as a function of $[CF_3]_0$ for laser experiments at various substrate temperatures. $[CF_3]_0$ was varied by changing $F^i_{CF_3I}$ from 1×10^{15} to 1×10^{16} s^{-1}.

1. CF_3 recombination and k_w

As we pointed out in Sec. II, k_w, the net surface loss of CF_3 may be obtained from C_2F_6 yields via Eq. (5). In effect, this method of obtaining k_w corresponds to measuring the extent to which C_2F_6 formation departs from purely second-order behavior with respect to CF_3. The discrepancy is caused by CF_3 escape and surface loss, both of which are first order. Knowledge of k_r[15] (recombination) and k_e (escape) allow the determination of k_w.

Figure 8(a) shows the C_2F_6 results of Fig. 4 plotted in the form of Eq. (5). These data conform nicely to expression 5, giving linear plots with intercept 2.0 for all the temperatures studied. Table II summarizes the information obtained from these results. k_w is obtained from the slopes, using $k_r = 3\times10^{-12}$ cm^3 s^{-1} and k_e in expression (5). (k_r used in evaluating k_w was taken independent of the surface temperature because it is a gas phase reaction, whose temperature it governed by that of the vessel walls. Since the hot active surface constitutes only 5% of the reactor wall area, the correction would be small. Furthermore, the dependence of k_r on temperature is not very strong in this range.) Notice that k_w increases with increasing surface temperature indicating that increasing amounts of CF_3 are irreversibly lost in the surface reaction. An Arrhenius plot of ln k_w vs the reciprocal surface temperature is shown in Fig. 8(b), together with a least-squares fit. The resulting k_w is given by the following expression: $k_w = 10^{2.9} \exp(-4700/RT)$ s^{-1}, where $R = 1.987$ cal mol^{-1} K^{-1}.

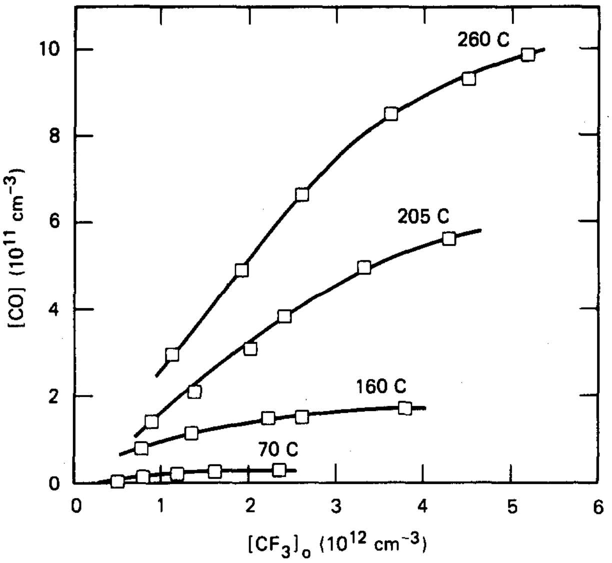

FIG. 5. $[CO]$ as a function of $[CF_3]_0$ for various substrate temperatures. Conditions are the same as in Fig. 4.

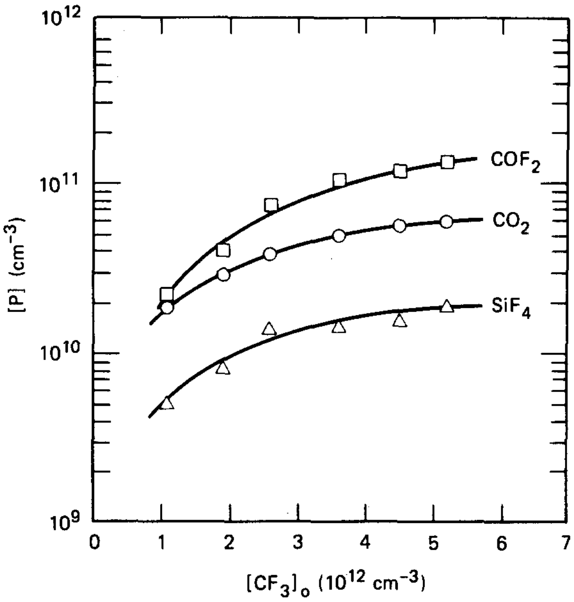

FIG. 6. $[SiF_4]$, $[CO_2]$, and $[COF_2]$ as functions of $[CF_3]_0$ for $T_{SiO_2} = 260$ °C. Conditions are the same as in Fig. 4.

Having determined k_w, we now know all of the rate constants in scheme (1)–(4), and therefore can obtain the steady-state CF_3 concentration:

$$[CF_3]_{ss} = \frac{-(k_e + k_w) + [(k_e + k_w)^2 + 8k_r f F^i_{CF_3I} V^{-1}]^{1/2}}{4k_r}. \qquad (6)$$

We find that $[CF_3]_{ss}$ is between 5% and 20% of $[CF_3]_0$ for the temperature range studied.

2. Formation of CO and k_{CO}

We have chosen the formation of CO as a marker for the surface reaction of CF_3 with H_2O. Figure 9 shows the data in Fig. 5 plotted as [CO] vs the steady-state CF_3 concentration, $[CF_3]_{ss}$. For all the temperatures, [CO] is linear with respect to $[CF_3]_{ss}$ and has no intercept, indicating a first-order reaction as would be expected from Eq. (4). The observed CO formation rate constant k_{CO} is obtained from the slope is each case (slope $= k_{CO}/k_e^{CO}$); these are given in Table II. The resulting k_{CO} can be represented by the following Arrhenius expression: $k_{CO} = 10^{3.7} \exp(-7500/RT)$ s^{-1} [Fig. 9(b)].

Notice in Table II that the k_{CO} rate constants are smaller than the corresponding k_w based on the loss of CF_3 on the heated fused silica surface. The latter indicates that not all the CF_3 that is lost to the surface from the gas phase [reaction (4)] proceed to form CO. This results in an appar-

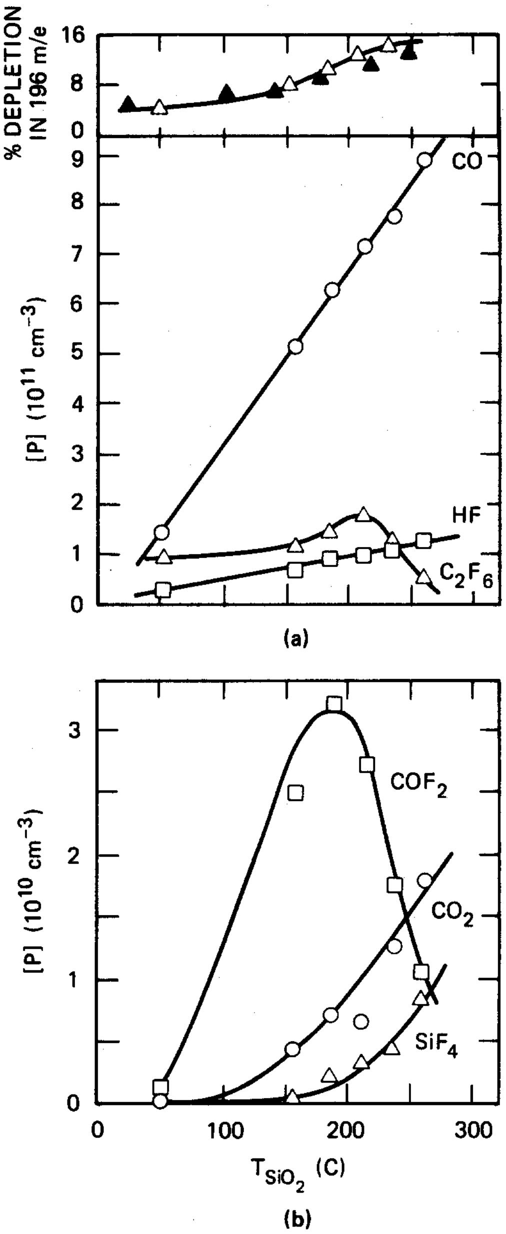

FIG. 7. Product concentrations as functions of T_{SiO_2} in laser experiments. (a) CO, HF, and C_2F_6. (b) COF_2, CO_2, and SiF_4. The inset shows f, the fractional depletion in CF_3I as a function of T_{SiO_2}; see the text for details. $F^i_{CF_3I} = 4.0 \times 10^{15}\ s^{-1}$.

ent excess of CF_3 on the surface, which must be removed by some other reaction.

The simplest mechanism that accommodates these results replaces Eq. (4) with Eqs. (4a), (4b), and (4c):

$$CF_3 + S \underset{k_d}{\overset{\beta\omega}{\rightleftarrows}} CF_3 - S\,, \tag{4a}$$

$$CF_3 - S \xrightarrow{k_1} CO\,, \tag{4b}$$

$$CF_3 - S \xrightarrow{k_2} \text{other products}\,. \tag{4c}$$

Equation (4a) represents adsorption and desorption of CF_3 where ω is the collision frequency of CF_3 with the active surface, β is the efficiency factor ($\beta<1$), and k_d is the rate constant for desorption. Reaction (4b) represents the formation of CO, and reaction (4c) corresponds to the sum of all those reactions that make up for the CO deficiency. The experimentally observed quantities k_w and k_{CO} may be expressed in terms of mechanism [4(a)–4(c)] as follows:

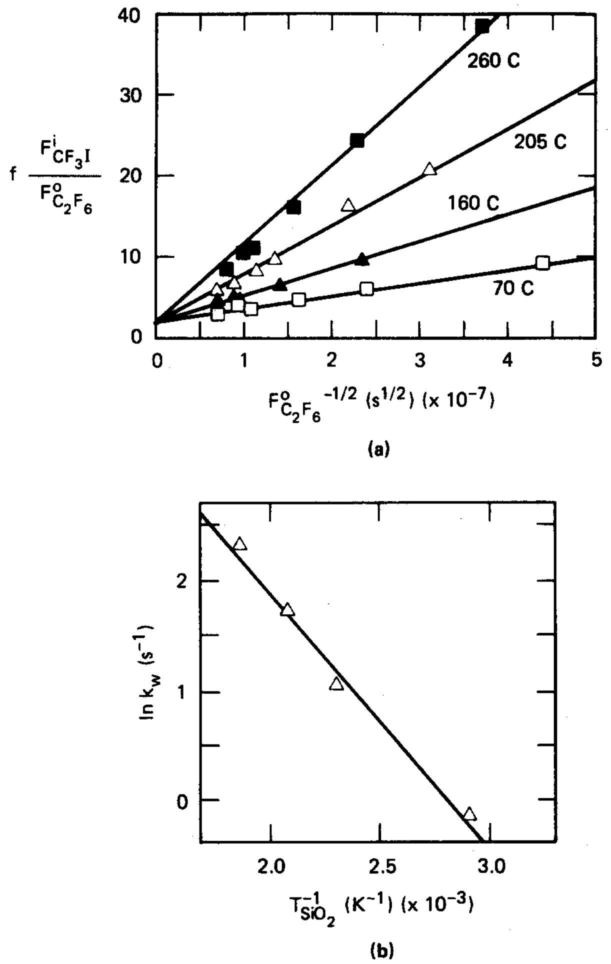

FIG. 8. (a) $fF^i_{CF_3I}/F^o_{C_2F_6}$ as a function of $F^o_{C_2F_6}{}^{-1/2}$ [see Eq. (5) in the text]. The straight lines correspond to least-squares fits to the data with intercept = 2.0. (b) ln k_w as a function of $T^{-1}_{SiO_2}$. The line is the linear least-squares fit, corresponding to $k_w = 10^{2.9} \exp(-4700/RT)$.

$$k_w = \frac{\beta\omega(k_1+k_2)}{(k_d+k_1+k_2)}\,, \tag{7}$$

$$k_{CO}\ (\text{observed}) = \frac{\beta\omega k_1}{(k_d+k_1+k_2)} = \frac{k_1}{(k_1+k_2)}\,k_w\,. \tag{8}$$

Using our measured k_{CO} and k_w, we obtain for the branching ratio,

$$\frac{k_1}{(k_1+k_2)} = 10^{0.8} \exp(-2800/RT)\,.$$

In relation to our experiments, Eq. (4c) may include the observed products CO_2 and COF_2. However, the latter can account for only 10% of the CO deficiency. Of course, Eq. (4c) may include reactions generating involatile products on the surface; these would not be determined by gas-phase analysis.

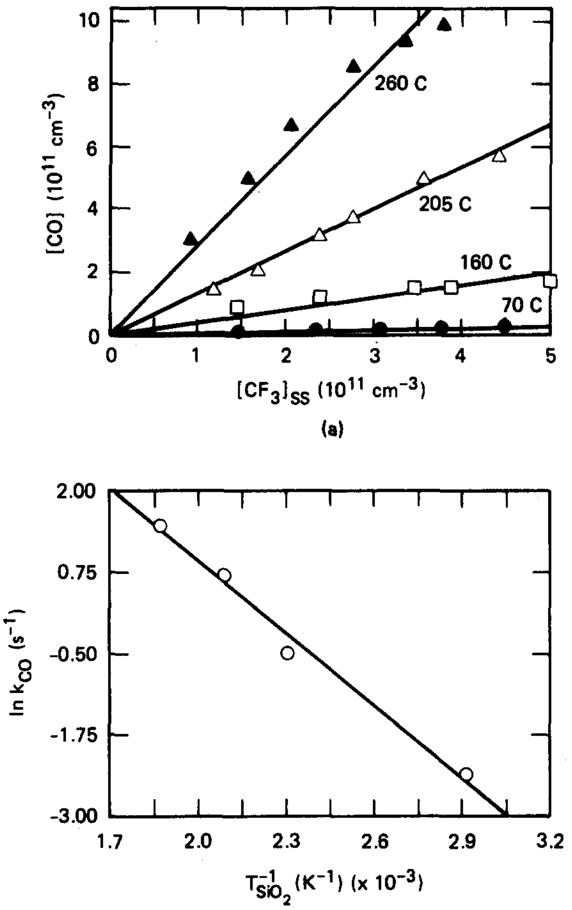

(a)

(b)

FIG. 9. (a) [CO] as a function of $[CF_3]_{ss}$. $[CF_3]_{ss}$ was obtained using Eq. (6) (see the text for details). The straight lines correspond to least-squares fits to the data with intercept 0. (b) ln k_{CO} as a function of $T^{-1}_{SiO_2}$. The line is the linear least-squares fit corresponding to $k_{CO} = 10^{3.7} \exp(-7500/RT)$.

3. CF_3 sticking coefficient on fused silica

γ, the sticking coefficient is given by k_w/ω where ω is the collision frequency of CF_3 with the silica surface. γ is the probability that a CF_3 impinging on this surface will be irreversibly lost. The values obtained for γ are listed in Table II. Notice that these are low, between 0.0014 and 0.017 depending on the temperature, in contrast to values in the literature, measured as 0.08–0.75 for CF_3 on *silicon* at room temperature.[16] In our case, a close-to-unity γ would have implied that the surface loss of CF_3 were competitive with ω. Since $\omega \sim 600$ s^{-1} and the time scale for gas-phase chemistry is in the order of seconds, negligible gas-phase reaction (i.e., recombination) would have been expected under conditions where $\gamma \sim 1$ and $k_w \sim \omega$. Our results indicate that this is not the case.

TABLE II. k_w, k_{CO}, and γ as functions of T_{SiO_2}.

T_{SiO_2} (C)	k_w (s^{-1})[a]	k_{CO} (s^{-1})[b]	γ[c]
70	0.85	0.103	0.0014
160	2.79	0.401	0.0047
205	5.87	2.16	0.0098
260	10.1	3.84	0.017

[a] Obtained from slopes in Fig. 8(a) using Eq. (5).

[b] Obtained from Fig. 9(a); slope = k_{CO}/k_e^{CO}.

[c] $\gamma = k_w/\omega$ where $\omega = 600$ s^{-1} for CF_3 collisions with the silica surface.

As a further test to confirm that γ is not close to unity, we carried out experiments where the gas-phase CF_3 radicals were trapped by Cl_2, yielding CF_3Cl. The resulting product yields vs Cl_2 flow rate are shown in Fig. 10. Notice that the surface reaction yielding CO is competitive with the gas-phase trapping reaction yielding CF_3Cl. Furthermore, behavior of the surface product CO resembles that of the gas-phase recombination product C_2F_6. That surface chemistry competes with gas-phase chemistry indicates once again that the surface reaction is slow compared to ω and that $\gamma \ll 1$.

The competition between the trapping reaction and the surface reaction may be seen more clearly by adding the trapping reaction (9) to the scheme depicted by Eqs. (1)–(4c):

$$CF_3 + Cl_2 \xrightarrow{k_T} CF_3Cl + Cl. \qquad (9)$$

Equation (9) represents one more loss process for the CF_3 radicals formed in the reactor, in addition to recombination, escape and surface loss. The rate of loss of CF_3 radicals from the gas phase, $k^{CF_3}_{loss}$, is given by

$$k^{CF_3}_{loss} = k_T[Cl_2] + k_r[CF_3] + k_e + \gamma\omega. \qquad (10)$$

Notice in Eq. (10) that the homogeneous Cl_2 trapping reaction is in direct competition with the CF_3 surface loss $\gamma\omega$, as well as with escape (k_e) and recombination ($k_r[CF_3]$). Varying $[Cl_2]$ allows for varying degrees of competition, as seen in Fig. 10. Notice that even a small concentration of Cl_2 affects both the recombination product C_2F_6 and the surface reaction product CO. The fact that the surface product yield is reduced by such a small amount of Cl_2 indicates that trapping by Cl_2 and the surface reaction are competitive, leading to $\gamma \ll 1$. Although the data shown in Fig. 10 may be modeled

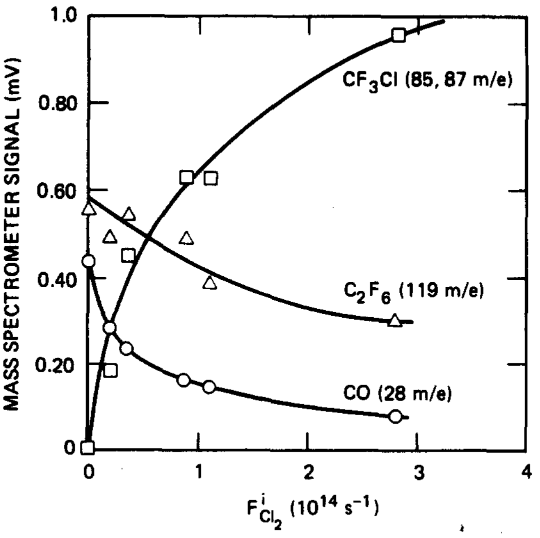

FIG. 10. Mass spectral signals of products CF_3Cl, CO, and C_2F_6 as functions of Cl_2 flow rate for trapping experiments. $F^i_{CF_3I} = 3.1 \times 10^{15}$ s^{-1}, $T_{SiO_2} = 110$ °C. $[Cl_2]$ (cm^{-3}) is given by $4.1 \times 10^{-3} F^i_{Cl_2}$ (s^{-1}).

by including reaction (9) in our earlier reaction scheme, this will have to wait for reliable values of k_T. However, the trapping experiments demonstrate the usefulness of our approach for obtaining γ.

IV. CONCLUSIONS

The present study reveals that the major reactivity of CF_3 radicals on the silica surface is with H_2O and not with SiO_2. Under these conditions, where H_2O is always present on the surface, the $CF_3 + SiO_2$ reaction accounts for only $\sim 1\%$ of the reactivity of CF_3 with H_2O. Added water inhibits the $CF_3 + SiO_2$ etching reaction even further. This is an important result that may be significant in applications. For example, presence of water in plasma etching systems may inhibit etching by radicals and may affect the final results. In the future, we plan to eliminate water in our experiments by using a stainless steel reactor and will then direct our attention to the $CF_3 + SiO_2$ reaction as well as other etching reactions.

It should be mentioned that we also investigated the reaction between CF_2 radicals and the SiO_2 surface. These were hot-wire experiments where CF_2HCl was decomposed, yielding CF_2 radicals. By contrast to our work with CF_3, we did not see any SiF_4, nor any other surface-related products in the CF_2 experiments. This result is in contrast to those of Brannon,[8] and of Loper and Tabat[4] who found that CF_2 radicals etched SiO_2 considerably while etching by CF_3 was not observed. In their experiments, the surface as well as the gas was irradiated. Recent results of Brannon[17] indicate that when the surface is not irradiated, CF_2 radicals do not etch SiO_2, but rather deposit onto the surface as a fluorocarbon layer. The latter results are compatible with our findings for CF_2. The fact that etching by CF_3 was not observed by either of the abovementioned workers may seem to contradict our results for CF_3. However, we suspect that under the experimental conditions of those studies, there may have been a negligible concentration of CF_3 radicals. In the case of Brannon's study,[8] CF_3 radicals were produced in a focused beam and the high intensities may have led to secondary decomposition of CF_3. In the work of Loper and Tabat,[4] where high pressures (50–100 Torr) were employed, it is possible that second-order recombination yielding C_2F_6 consumed most of the CF_3 radicals, so that etching by CF_3 was not observed.

Our results demonstrate that the VLPΦ method may be successfully used to study radical–surface reactions. Not only qualitative information on gas-phase products, but also quantitative information on the reaction kinetics may be obtained. The technique allows for determination of the order of the surface reaction, the rate constant and its temperature dependence, and also, k_w, the surface loss constant for the reactive radical. Knowledge of k_w leads directly to γ, the sticking coefficient for the radical of interest.

In future experiments, we plan to extend the technique to include *in situ* detection of radicals by multiphoton ionization. This will allow for the determination of local real-time concentrations of radicals within the reactor. In addition to gas-phase product analysis, we also plan to probe the surface using surface analysis techniques, such as SALI (surface analysis by laser ionization) recently developed at SRI.[18]

[1] J. W. Coburn, Plasma Chem. Plasma Proc. **2**, 1 (1982).

[2] D. L. Flamm, V. M. Donnelly, and D. E. Ibbotson, J. Vac. Sci. Technol. B **1**, 23 (1983).

[3] J. W. Coburn and H. F. Winters, J. Vac. Sci. Technol. **16**, 391 (1979).

[4] G. L. Loper and M. D. Tabat, *Proceedings of the International Conference on Lasers '83*, edited by R. C. Powell (STS, McLean, VA, 1983).

[5] D. L. Flamm, C. J. Mogab, and E. R. Sklaver, J. Appl. Phys. **50**, 6211 (1979).

[6] H. F. Winters and F. A. Houle, J. Appl. Phys. **54**, 1218 (1983).

[7] G. L. Loper and M. D. Tabat, Appl. Phys. Lett. **46**, 654 (1985).

[8] J. H. Brannon, J. Phys. Chem. (to be published).

[9] J. W. Coburn, H. F. Winters, and T. J. Chuang, J. Appl. Phys. **48**, 3532 (1977).

[10] S. C. McNevin and G. E. Becker, J. Vac. Sci. Technol. B **2**, 27 (1984).

[11] M. J. Rossi, J. R. Barker, and D. M. Golden, J. Chem. Phys. **71**, 3722 (1979).

[12] D. M. Golden, M. J. Rossi, A. C. Baldwin, and J. R. Barker, Acc. Chem. Res. **14**, 56 (1981).

[13] M. J. Rossi and D. M. Golden, Int. J. Chem. Kinet. **15**, 1283 (1983).

[14] A. C. Baldwin and D. M. Golden, J. Geophys. Res. **85**, 2888 (1980).

[15] k_r, the gas-phase CF_3 recombination rate constant, was investigated in separate experiments. These were performed using the same VLPΦ reactor, but in the absence of the active fused silica surface. Measurements with two sizes of escape apertures allowed the determination of k_r, as well as possible loss, k_w, on the gold-coated walls. These yielded $k_r = 3\times10^{-12}\ \mathrm{cm}^3\ \mathrm{s}^{-1}$ and very small wall loss $k_w \sim 0.04\ \mathrm{s}^{-1}$. [N. Selamoglu, M. J. Rossi, and D. M. Golden, Chem. Phys. Lett. (to be published)].

[16] H. F. Winters, J. Appl. Phys. **49**, 5165 (1978).

[17] J. H. Brannon (private communication).

[18] C. H. Becker and K. T. Gillen, Anal. Chem. **56**, 1671 (1984).